Biomaterials 35 (2014) 9888–9896

Contents lists available at ScienceDirect

Biomaterials

journal homepage: www.elsevier.com/locate/biomaterials

A platform technique for growth factor delivery with novel mode of action

Nam Hee Kim [a, 1], Yong Hoon Cha [a, 1], Hyun Sil Kim [a], Soo Eon Lee [b], Jong-Ki Huh [c], Jung Kook Kim [d], Jeong Moon Kim [d], Joo Kyung Ryu [a], Hee-Jin Kim [e], Yoonmi Lee [a], Su Yeon Lee [f, g], Insup Noh [f, g], Xiao-Yan Li [h], Stephen J. Weiss [h], Tae-Ahn Jahng [b, *], Jong In Yook [a, *]

[a] Department of Oral Pathology, Oral Cancer Research Institute, Yonsei University College of Dentistry, Seoul 120-752, South Korea
[b] Department of Neurosurgery, Seoul National University College of Medicine, Seoul 110-799, South Korea
[c] Department of Oral and Maxillofacial Surgery, Yonsei University College of Dentistry, Seoul 120-752, South Korea
[d] Orthotion, 104 Suntechcity, 513-15, Sangdaewon-dong, Joongwon-gu, Seongnam-si, Kyunggi-do 462-725, South Korea
[e] Department of Anatomy, Yonsei University College of Dentistry, Seoul 120-752, South Korea
[f] Department of Chemical Engineering, Seoul National Universtiy of Science and Technology, Seoul 139-743, South Korea
[g] Convergence Institute of Biomedical Engineering and Biomaterials, Seoul National University of Science and Technology, Seoul 139-743, South Korea
[h] Division of Molecular Medicine and Genetics, Department of Internal Medicine and the Life Sciences Institute, University of Michigan, Ann Arbor, MI 48109, USA

ARTICLE INFO

Article history:
Received 26 June 2014
Accepted 1 August 2014
Available online 15 September 2014

Keywords:
Protein transduction domain (PTD)
Mode of action (MoA)
Growth factors
Regenerative medicine

ABSTRACT

Though growth factors allow tissue regeneration, the trade-off between their effectiveness and adverse effects limits clinical application. The key issues in current growth factor therapy largely derive from initial burst pharmacokinetics, rapid clearance, and proteolytic cleavage resulting in clinical ineffectiveness and diverse complications. While a number of studies have focused on the development of carriers, issues arising from soluble growth factor remain. In this study, we report a prodrug of growth factors constituting a novel mode of action (MoA). To mimic endogenous protein processing in cells, we developed a recombinant BMP-2 polypeptide based on a protein transduction domain (PTD) to transduce the protein into cells followed by furin-mediated protein cleavage and secretion of active growth factor. As proof of concept, a few micrograms scale of PTD-BMP-2 polypeptide sufficed to induce bone regeneration in vivo. As a simple platform, our technique can easily be extended to delivery of BMP-7 and DKK-1 as therapeutics for TGF-β and canonical Wnt signaling, respectively, to suppress the epithelial–mesenchymal transition (EMT), which constitutes a fundamental biological mechanism of many diseases. This technique largely overcomes the limitations of current soluble growth factors and opens the door to next generation growth factor therapeutics.

1. Introduction

The mode of action (MoA) of the soluble growth factors is simply to interact with membrane receptors on target cells, thereby triggering an intracellular signaling cascade for regeneration. Since their approval by the FDA several decades ago, the recombinant bone morphogenic proteins (rhBMPs) have been widely studied for use in bone regeneration. Though the BMPs were initially identified as osteoinductive factors present in demineralized bone matrix [1,2], it is now evident that the BMP family induces mesenchymal-to-epithelial reversion, a major therapeutic goal in treating cancer progression and degenerative disorders [3]. For example, BMP-7 has been identified as an endogenous antagonist of TGF-beta mediated EMT in the kidney and other organs [4–6]. Administration of recombinant BMP-7 in mice with renal fibrosis resulted in reversal of EMT and repopulation of healthy tubular epithelial cells with functional recovery though the current technique for BMP-7 delivery to large visceral organs is very limited [4,6,7]. The insulin-like growth factors, granulocyte–macrophage colony stimulating factor, basic fibroblast growth factor, and platelet-

* Corresponding authors.
E-mail addresses: taj@snu.ac.kr (T.-A. Jahng), jiyook@yuhs.ac (J.I. Yook).
[1] NHK and YHC contributed equally to this work.

http://dx.doi.org/10.1016/j.biomaterials.2014.08.005
0142-9612/

derived growth factor have all demonstrated potential for use in regenerative therapy [8].

Despite extensive research into the safety and efficacy of the growth factors in both animal and clinical trials, many complications remain, including ectopic bone formation, osteolysis, pain, and swelling [9,10]. Considering the long-term regeneration process in vivo, it is difficult to resolve the dilemma between efficacy and adverse effects with respect to direct MoA of soluble factors exhibiting an initial burst release pharmacokinetic profile [11]. Because of the short half-life of rhBMP, mainly due to rapid clearance and enzymatic degradation [11,12], excess dosage of soluble proteins, even mg scale (one million times the concentration needed for physiologic regeneration), is often applied to ensure clinical effectiveness. However, high doses of soluble growth factors inevitably increase the chance of diffusion to nearby tissues or blood circulation, with many adverse effects [9,13]. Although many carriers have been adapted for controlled release to overcome the initial burst and rapid clearance rate, the mutual exclusivity between safety and efficacy remains. The cost-effectiveness and legal issues related to soluble recombinant growth factors currently pose a challenge in many medical indications [14,15].

The cell-permeable, protein transduction domain (PTD) peptides have been found to transduce protein across the plasma membrane into the cell as part of a physiologic process [16]. The PTD is widely studied for delivery of macromolecules such as peptides, catalytic proteins, and oligonucleotides [17], providing a therapeutic advantage without raising the safety issues associated with gene delivery. Following initial ionic contact with the cell membrane, PTD-fusion polypeptide is rapidly internalized by lipid raft-dependent macropinocytosis independent of specific receptors [18]. Interestingly, the denatured polypeptides delivered into cells are refolded and elicit physiological protein function in cells and in vivo [19,20], though the mechanism of intracellular processing of delivered protein is still not fully defined [19–21]. Thus, we adopted the PTD technique for post-translational processing and secretion of growth factors mimicking endogenous protein biogenesis to overcome an intrinsic limitation of soluble factor therapy using an indirect MoA. The transduced TAT-BMP-2 polypeptide was properly processed in a furin-dependent manner and secreted as bioactive BMP-2. The hydrogel composite with the polypeptide was functional to promote bone regeneration as proof of concept in vivo. In addition to resolving the issue of initial burst release, the technique was easily extended to BMP-7 and Wnt antagonist Dickkopf-1 (DKK-1), providing a platform for delivery of therapeutic secreted proteins in regenerative medicine.

2. Materials and methods

2.1. Bacterial expression constructs and protein purification

The bacterial expression cassette for PDT-fusion polypeptide was constructed based on pRSET bacterial expression vector (Invitrogen) having His purification tag and Xpress epitope. The TAT sequences (RKKRRQRRR) for the PTD domain were inserted next to the epitope and the precursor cDNAs of BMP-2, BMP-7, or DKK-1 were cloned into a TAT-expression cassette. The precursor cDNA of BMPs and DKK-1 were obtained by PCR amplification of cDNA of Saos-2 osteosarcoma cells and 293T cells, respectively. The TAT sequence was omitted for negative control of protein transduction. Mutant expression vectors for BMP-2 were constructed by deletion of signal peptide (aa 1–24), prodomain (aa 1–270), or mutation of furin cleavage site of REKR to REKA (aa 279–282). Induction and purification of the recombinant protein were followed as described by Dowdy's group [19,22]. Briefly, following transformation of BL21 and IPTG induction, the inclusion bodies were obtained from insoluble fraction of 1% Triton X-100 buffer. The insoluble fraction was solubilized with 8 M urea solution and the recombinant protein purified with Ni–Ti beads and imidazole elution followed by buffer shock to gain high surface energetic (ΔG) properties.

2.2. Cells, western blot analysis, cell migration assay, and immunofluorescence

The murine C3H10T1/2 and osteoblast precursor cell line MC3TC were obtained from ATCC (CCL-226) and culture following manufacturer's recommendations. MCF-7, A549, and 293 cells were described previously [23]. The recombinant protein was directly applied to regular or serum-free culture medium (Opti-MEM) in the indicated amount. The soluble and insoluble fractions of lysate were obtained from Triton X-100 lysis buffer. To detect transduced recombinant protein in cells, the whole fractions of cell were prepared in SDS-RIPA buffer followed by heating at 95 °C for 5 min. The commercially available primary antibodies were directed against anti-Xpress (Invitrogen), BMP-2 (R&D systems), Tubulin (Labfrontier), α1-antitrypsin (Sigma), Snail (Cell Signaling), β-catenin (R&D systems), and E-cadherin (Invitrogen). Cell migration potential of A549 cells was evaluated by transwell assay as described previously [24]. Mammalian expression vector for α1-antitrypsin Portland (α1PDX) was described previously [25]. For immunofluorescent analysis, the cells were treated with TAT-BMP for 1 h and the transduction of recombinant protein was detected against anti-Xpress monoclonal antibody and anti-mouse IgG-conjugated Alexa-Fluor-488 secondary antibody as described previously [23].

2.3. RT-PCR for cbfa-1/Runx2

The murine C3H10T1/2 cells were treated with TAT-BMP-2 for a 16 h culture period and total RNA was harvested with Trizol. The cDNA was synthesized with random hexamer and routine RT-PCR performed. The primer sequences for mouse cbfa-1 and GAPDH of control were as follows: cbfa-1, forward, 5′-ctcttcccaaagccagagtg; cbfa-1, reverse, 5′-cagcgtcaacaccatcattc; mouse GAPDH, forward, 5′-tgaaggtcggagtcaacggattt; GAPDH, reverse, 5′-catgtgggccatgaggtccaccac.

2.4. ELISA assay BMP, alkaline phosphatase, and mineralization assay

To detect secreted BMP-2, 100 ng of recombinant protein were transduced into the 293 cells for 2 h followed by PBS washing and refreshment of serum-free Opti-MEM medium (300 μl in 6-well plate). After 4 h of incubation, the cell lysates and culture medium were harvested. Fifty μl of lysates or culture medium were subjected to ELISA assay for BMP-2 (R&D systems) according to the manufacturer's protocol. Commercially available recombinant BMP-2 (R&D systems) was used as control for the quantitation. To detect alkaline phosphatase activity in cells, a commercially available kit (Wako) was used following the manufacturer's instructions. C3H10T1/2 cells at the late log phase of growth were treated with 10 ng of TAT-BMP-2 or 10 ng of rhBMP-2 (R&D systems) or negative control, and the cells maintained for 4 days before the alkaline phosphatase assay. For mineralization assay of C3H10T1/2 cells, an osteogenesis assay kit (Millipore) based on Alizarin Red S stain was used. The cells were treated with recombinant proteins or negative control for 2 h and the cells incubated in osteogenic culture medium for 14 days. Treatment with the recombinant protein was repeated every 2 days for mineralization assay.

2.5. Furin cleavage assay

Ten units of human recombinant furin (Sigma) were subjected to protein cleavage of the full-length or mutant TAT-BMP-2 protein followed by immunoblot analysis. For in vitro furin cleavage analysis, soluble fractions of recombinant protein were used, the cleaved protein being detected by immunoblot analysis using anti-BMP-2 antibody.

2.6. Reporter assay of E-cadherin, Wnt/TCF, and TGF-β responsive activity

The Wt and E-box mutated E-cadherin proximal reporter constructs (nt-108 to +125) were used as described previously [26]. The luciferase reporter of Topflash (TCF/LEF binding sites upstream of a luciferase reporter), FOPflash (mutated TCF/LEF binding sites), and 3 TP-lux having Smad-binding site on plasminogen activator inhibitor-1 (PAI-1) promoter were obtained from Addgene. The cells were transiently transfected with 100 ng of reporter constructs and 2 ng pSV-Renilla using Lipofectamine2000 (Invitrogen). After 24 h of transfection, the culture medium was refreshed with or without recombinant protein as indicated. The relative ratio of Renilla to firefly luciferase after a 48 h transfection period was determined by dual-luciferase assay kit (Promega) from triplicate experiments.

2.7. Hydrogel preparation and biocompatibility test on HA hydrogel

Hydrogel for animal experiments was prepared from low molecular weight hyaluronic acid (low HA, MW 340kd) as described previously [27]. Briefly, low HA was reacted with adipic acid dihydrazide using N-(3-diethylpropyl)-N-ethylcarbodiimide (EDC) as a cross-linking agent at room temperature to synthesize HA-ADH. HA polymers of HA-Ac and HA-TCEP were prepared from HA-ADH through a reaction with acrylic acid (Ac) or tris(2-carboxyethyl)phosphine (TCEP), respectively. The obtained polymers of HA-Ac and HA-TCEP were precipitated with 95% EtOH and dialyzed for 3 days to remove unbound chemicals followed by freeze drying. Two separated 5% HA-Ac and HA-TCEP solutions were prepared in PBS. After separately sterilizing the HA-Ac and HA-TCEP solutions with a 0.2 μm syringe filter, TAT-BMP-2 was added to the HA-AC solution and hydrogel (HG) was synthesized by mixing the obtained solutions of HA-TCEP and HA-Ac with TAT-BMP-2 on culture plate. Cell culture on HG was performed by seeding MC3T3 cells on the surface of HG for 8 weeks. Cell adhesion and

proliferation were quantitatively measured with Cell Counting kit-8 (Dojindo). To evaluate osteoblastic differentiation in vitro by TAT-BMP-2, the MC3T3 cells were seeded and cultured on HG containing different doses of TAT-BMP2. The HG with cells was maintained for 8 weeks and subjected to routine immunohistochemical staining with Osteocalcin.

2.8. Animal study, microCT (microcomputed tomogram), and histomorphometric analysis

All animal handling and surgical procedures were conducted according to Seoul National University guidelines for the care and use of large laboratory animals, the study having been approved by the IACUC of Seoul National University Hospital Biomedical Research Institute (12-2011-000-05). Six female adult beagle dogs, weighing between 13 and 14 kg, were used in this study. Following routine premedications including antibiotic coverage, general anesthesia was maintained by intratracheal intubation with isoflurane and oxygen. The periosteum of the femur shaft was exposed via lateral approach and an electric drill (diameter 5.0 mm) used to place the cylinder-shaped HG (diameter 5 mm, length 6 mm; 177 mm^3), prepared prior to surgical procedures containing 2.5 μg of TAT-BMP or the same volume of PBS. Following careful placement of HG, the wounds were closed using routine procedures and protected using a Robert–Jones bandage until day 7. Five weeks post-operation, the femurs were dissected after euthanasia and fixed in 10% neutralized buffered formalin. The fixed specimens were subjected to microCT analysis (SkyScan 1076). Axial images of 200 μm cut were obtained and the raw data was converted to DICOM format for rendering through Simplant Crystal (Materialise). Regenerated bone volume was obtained from the 3-dimensional images with Simplant Pro Crystal software for the Intel X86 Platform, v13.0.1.4 (Materialise). Following microCT analysis, the specimens were subjected to routine decalcification. Paraffin-embedded sections were stained with Hematoxylin/Eosin and examined using light microscopy. Digital images from stained sections were processed with SPOT version 4.5 (Diagnostic Instruments) to calculate the regenerated bone area. The data was presented as mean ± standard error of the mean. Statistical analysis was conducted with SPSS 12.0 using *t*-test.

2.9. Chick CAM (chorioalantoic membrane) invasion assay

Invasive MDA-MB-231 cancer cells, labeled with dsRed by lentiviral transduction, were treated with fresh culture medium containing 500 ng of TAT-DKK1 1 h prior to CAM experiment. Non-treated cells or TAT-DKK1 transduction cells were cultured on the CAM of 11-d-old, live chicken embryos for 2 days as described previously [26,28]. Following DAPI (4′,6-diamidino-2-phenylindole) staining in cross-sections of the fixed CAM, invasion of labeled cancer cells was monitored by fluorescence microscopy. Invasive cells were counted in 10 high-power fields from triplicated samples.

2.10. Statistical analysis

All results were expressed as the mean SEM of three of more experiment unless indicated otherwise. *marks $p < 0.05$ and ** indicates $p < 0.01$.

3. Results

3.1. Design of experiment and transduction of PTD-BMP-2 fusion polypeptide

To overcome the initial burst of growth factors, we designed an indirect delivery system of BMP-2 using PTD-mediated recombinant protein as a prodrug of BMP (Fig. S1A). In this strategy, the recombinant polypeptide is transduced into the cells independently of its receptor followed by protein refolding, post-translational cleavage, and secretion of active BMP-2. We cloned cDNA of human BMP-2 into the bacterial expression cassette, then added PTD, epitope tag, and purification tag (Fig. 1A). We chose the HIV-derived cationic TAT (trans-activator of transcription) as a PTD as it is the most widely studied [29]. The TAT sequence was omitted

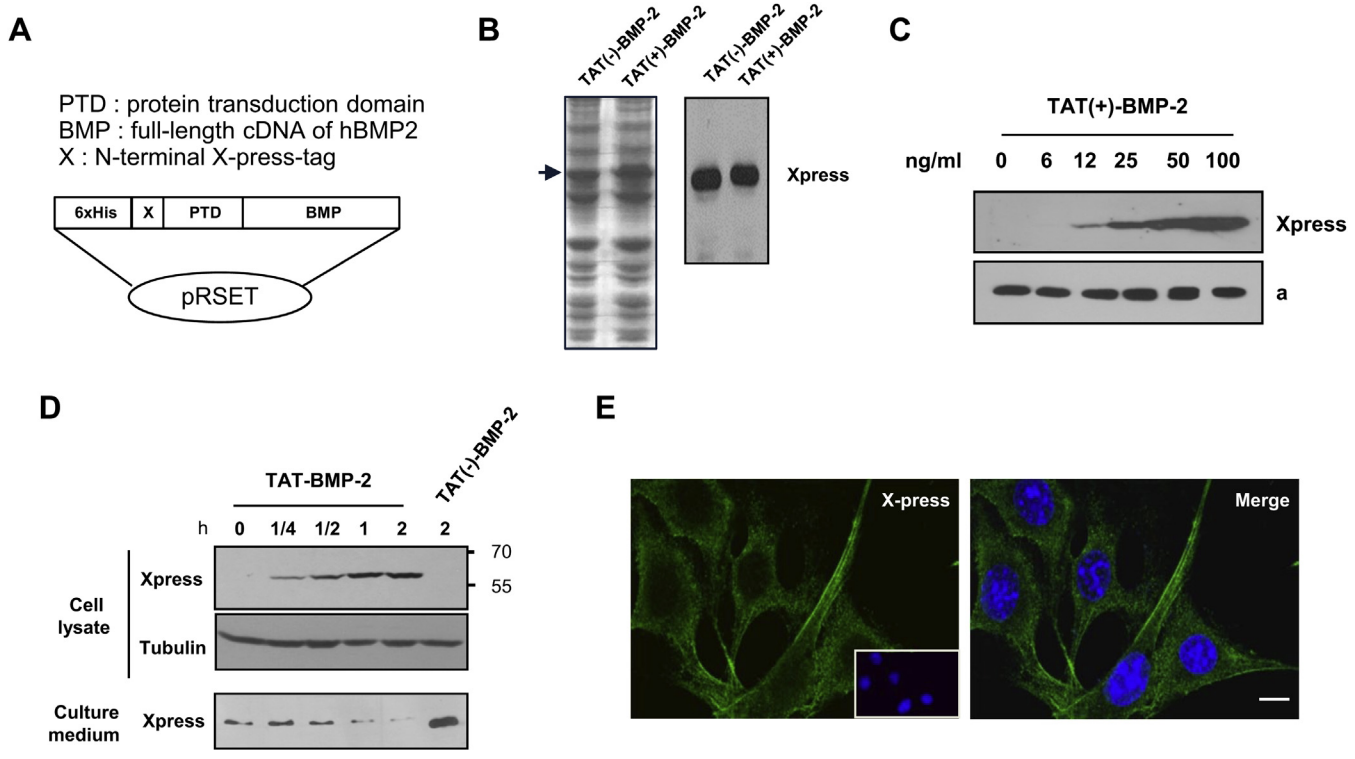

Fig. 1. Transduction of TAT-BMP-2 and secretion of BMP-2 in cells. (A) Schematic diagram of bacterial expression vector (pRSET) for TAT-BMP-2. The expression cassette contains 6× His tag for purification, PTD domain, X-press tag, and full-length hBMP-2 cDNA. (B) Induction of recombinant protein in bacteria, and Coomassie blue stained gel of crude lysates of bacteria (left panel). Arrow indicates bands of recombinant protein. Immunoblot analysis of purified recombinant protein detected by anti-Xpress tag (right panel). (C) C3H10T1/2 cells were treated with different doses of TAT-BMP-2 for 2 h; immunoblot analysis of whole cell SDS-RIPA lysate shows dose-dependent transduction of TAT-BMP-2. (D) Transduction of TAT-BMP-2 into cells in a time-dependent manner. Total protein containing insoluble fraction (cell lysate) and serum-free culture medium were subjected to immunoblot analysis to detect transduction of recombinant TAT-BMP-2 in C3H10T1/2 cells. The recombinant protein lacking PTD domain, labeled TAT(−)-BMP-2, was used for negative control of protein transduction. (E) The cells were transduced with 100 ng of TAT-BMP-2 and the transduction of recombinant protein (green) was determined by confocal laser microscopy. Nuclei are stained blue with ToTo-3 (inset in left panel). The scale bar in the merged image represents 10 μm.

as a negative control for protein transduction. Considering post-translational processing by proprotein convertase cleavages on the TGF/BMP family [30], we cloned the full-length cDNA precursor of BMP-2, having a signal peptide, prodomain, and mature BMP-2. For macropinosomal escape after transduction of the lipid bilayer, the HA2 domain was inserted between PTD and BMP-2 [18,31]. The denatured TAT fusion polypeptide was purified from inclusion bodies of transformed BL21 [19], then verified with gel staining and immunoblot analysis (Fig. 1B). Consistent with previous findings [17–19], the TAT-fusion BMP-2 polypeptide (TAT-BMP-2) was successfully delivered into cells from the culture medium regardless of cell type in a time- and concentration-dependent manner, whereas TAT-omitted negative control proteins were not (Fig. 1, C and D; Fig. S1B). Immunofluorescence study showed that the TAT-fusion protein is mainly localized in cytoplasm (Fig. 1E), indicating that the TAT-BMP-2 is successfully transduced into cells in a PTD-dependent manner.

3.2. Secretion of mature BMP-2 following transduction of TAT-BMP-2 polypeptide

Next, we examined whether the transduced recombinant TAT-BMP-2 was adequately processed and secreted. The transduced TAT-BMP-2 gradually disappeared from the insoluble fraction of cells in a time-dependent manner, indicating rapid processing of the transduced polypeptide (Fig. S1C). To exclude the possibility of protein degradation rather than intracellular processing and subsequent secretion, we examined the secreted BMP-2 following TAT-BMP-2 transduction. Interestingly, mature BMP-2 was detected mainly in culture medium after treatment of TAT-BMP-2 followed by incubation (Fig. 2A). Because the initially transduced TAT-BMP-2 was ~60 kd in molecular weight, we evaluated the molecular weight of secreted BMP-2 with immunoblot analysis. Secreted BMP-2 of ~15 kd was also successfully detected in culture medium when we specifically added Noggin, an endogenous inhibitor which blocks BMP binding to the cognate receptor on cell membrane (Fig. 2B). These results suggest that transduced TAT-BMP-2 was rapidly processed and secreted. To prove the recombinant polypeptide was functional on osteoblastic differentiation in vitro, we treated C3H10T1/2 cells with TAT-BMP-2 and examined the transcript abundance of Runx2/Cbfa1, an osteoblast-specific transcription factor. Indeed, pg level of the recombinant protein is sufficient to increase abundance of Runx2/Cbfa1 transcripts (Fig. 2C). Furthermore, the induction capacity of alkaline phosphatase activity and mineralization of C3H10T1/2 cells by TAT-BMP-2 transduction were comparable to rhBMP-2 in vitro (Fig. 2, D and E). These results indicate that TAT-BMP transduced into the cells successfully processed and secreted active BMP-2 in vitro.

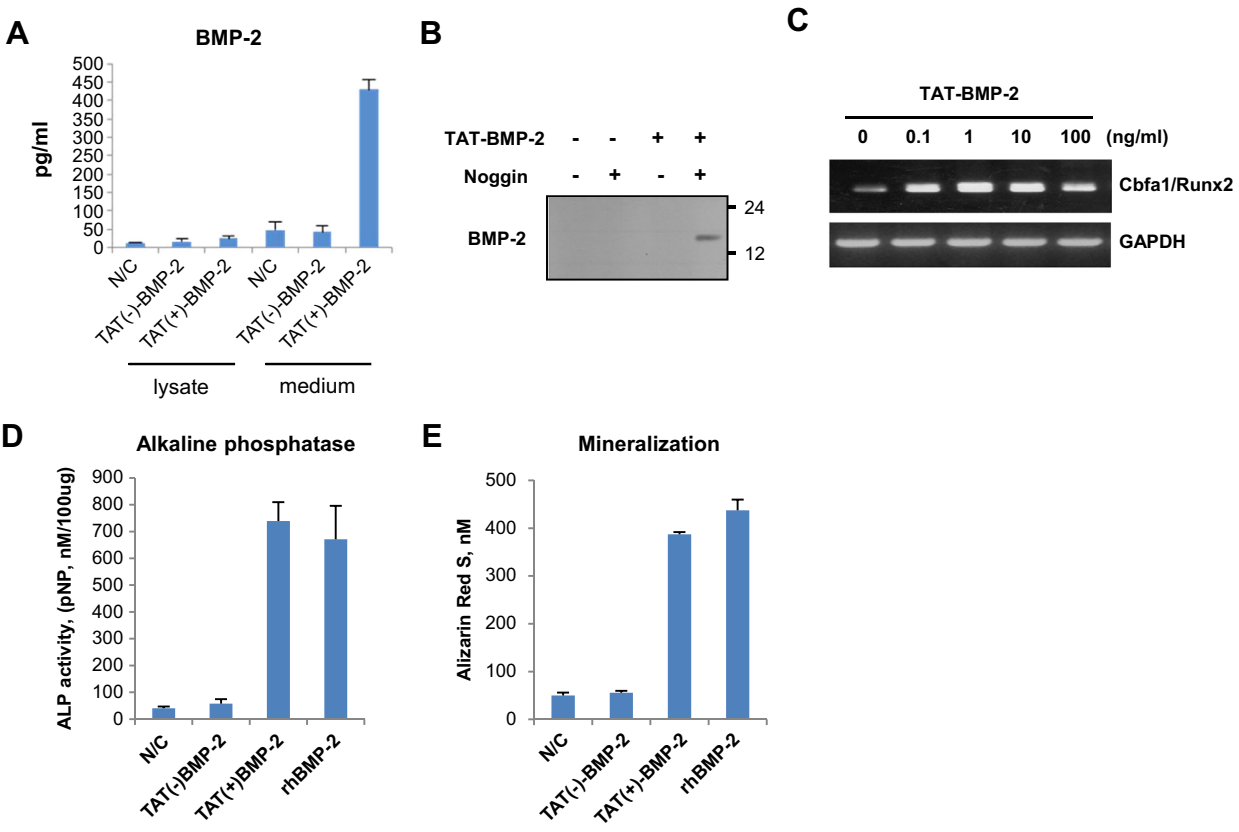

Fig. 2. Secretion of active BMP-2 following TAT-BMP-2 transduction. (A) The cells were treated with 500 ng of recombinant protein and the BMP-2 level was determined from the soluble cell lysates and culture medium as described in Methods. (B) Following transduction of TAT-BMP-2, the cells were incubated with serum free medium for 6 h. The soluble proteins in culture medium were precipitated with trichloroacetic acid, and secreted BMP-2 was determined by immunoblot analysis. The secreted BMP-2 in culture medium was precipitated with trichloroacetic acid and the precipitates were subjected to immunoblot analysis against anti-BMP-2 antibody. The recombinant Noggin (2 μg/ml) was used to inhibit BMP-2 binding to its cognate receptors. (C) The C3H10T1/2 cells were transduced with TAT-BMP-2 and the transcript level of cbfa-1/Runx2 was assessed by RT-PCR analysis. GAPDH was used for loading control. (D) C3H10T1/2 cells were transduced with 10 ng of TAT-BMP-2 and the alkaline phosphatase activity was measured. The same amount of recombinant protein omitting PTD domain and commercial rhBMP-2 were used for negative and positive control, respectively. (E) The cells were treated with 10 ng of TAT-BMP-2 or rhBMP-2 for 14 days, mineralization being determined by Alizarin Res S stain.

3.3. Intracellular processing of TAT-BMP-2 is critical for secretion of active BMP-2

The biologically active BMPs and other secreted proteins are derived from precursor polypeptides by post-translational processing of Furin/SPC-mediated endoproteolytic cleavage in the trans-Golgi network [25,30,32]. When we overexpressed furin inhibitor α1-PDX (α_1-antitrypsin Portland), an engineered variant of antitrypsin [33], renaturation of transduced TAT-BMP-2 in cells was delayed (Fig. 3A), suggesting that proteolytic cleavage by furin is required for intracellular processing of the recombinant protein. To further examine the role of endopeptidase cleavage on TAT-BMP-2, we made several mutants of TAT-BMP-2 by deleting the signal peptide or mutating the furin cleavage site and subjected the proteins to in vitro cleavage experiments (Fig. 3B). Indeed, furin treatment cleaved recombinant TAT-BMP-2 having wild type (wt) precursor, but not the mutants of prodomain deletion or cleavage site (Fig. 3C). Notably, deletion of the signal peptide on the N-terminus did not affect the proteolytic cleavage of TAT-BMP-2. Consistent with in vitro cleavage, the secretion of active BMP-2 in cells depended on the proteolytic processing of TAT-BMP-2 (Fig. 3D), indicating that furin cleavage is critically required for secretion of active BMP-2 following TAT-BMP-2 transduction.

3.4. TAT-BMP-2 is functional for in vivo bone regeneration

Given the well-known function of BMP-2 in bone regeneration, we designed a bone defect model of a mammal to examine the in vivo proof of concept of TAT-BMP-2 polypeptide. Considering that recombinant protein requires sustained release for several weeks in vivo, we chose a self-linking hyaluronic acid hydrogel (HG) because it is biodegradable, allowing controlled release of entrapped recombinant polypeptide to surrounding progenitor cells. The cellular biocompatibility and osteogenic differentiation potential of HG containing TAT-BMP-2 were verified in vitro, revealing that TAT-BMP-2 in HG scaffold increased cell proliferation of pro-osteoblastic cells and induced osteogenic differentiation (Fig. S2). Following the surgical procedure on dog femur, we placed

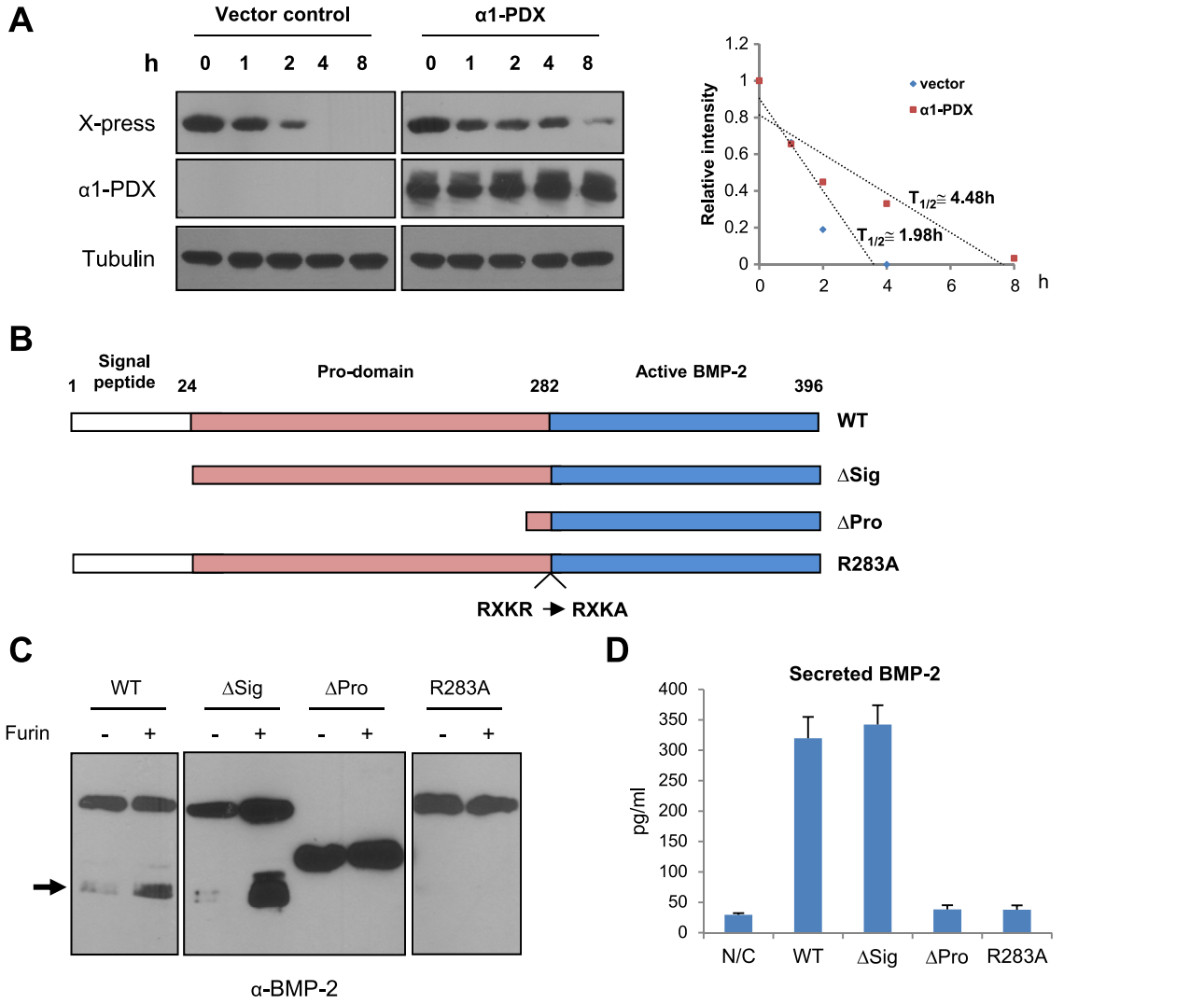

Fig. 3. Posttranslational cleavage by furin is essential for intracellular processing of TAT-BMP-2 and secretion of BMP-2. (A) Insoluble full-length protein level was chased after transduction of TAT-BMP-2 by immunoblot analysis in 293 cells transfected with control vector or α-1-PDX expression vector (left panels). Tubulin was used as the loading control. Protein half-life ($T_{1/2} = -0.5$/slope) was obtained by densitometric analysis (right panel). (B) Schematic diagram of recombinant proteins to examine furin cleavage. (C) The soluble recombinant proteins of wt or mutant BMP-2 were subjected to proteolytic cleavage assay and the cleaved BMP-2 (arrow) was determined by immunoblot analysis. (D) The C3H10T1/2 cells were transduced with 100 ng of wt or mutant TAT-BMPs and secreted BMP-2 levels were determined by ELISA assay from culture medium. Commercial rhBMP-2 was used for standardized quantitation.

HG containing 2.5 μg of TAT-BMP-2 polypeptide into the bone defects for 5 weeks. Examining osteogenic potential with microCT, we found that the HA gel with TAT-BMP-2 significantly increased bone regeneration compared to the HA gel control in terms of mineralized area and bone density (Fig. 4, A and B). Histological examination further showed bone defects delivering TAT-BMP-2 being filled with dense mature bone trabecular in contrast to limited regeneration with fibrous stroma in the control group

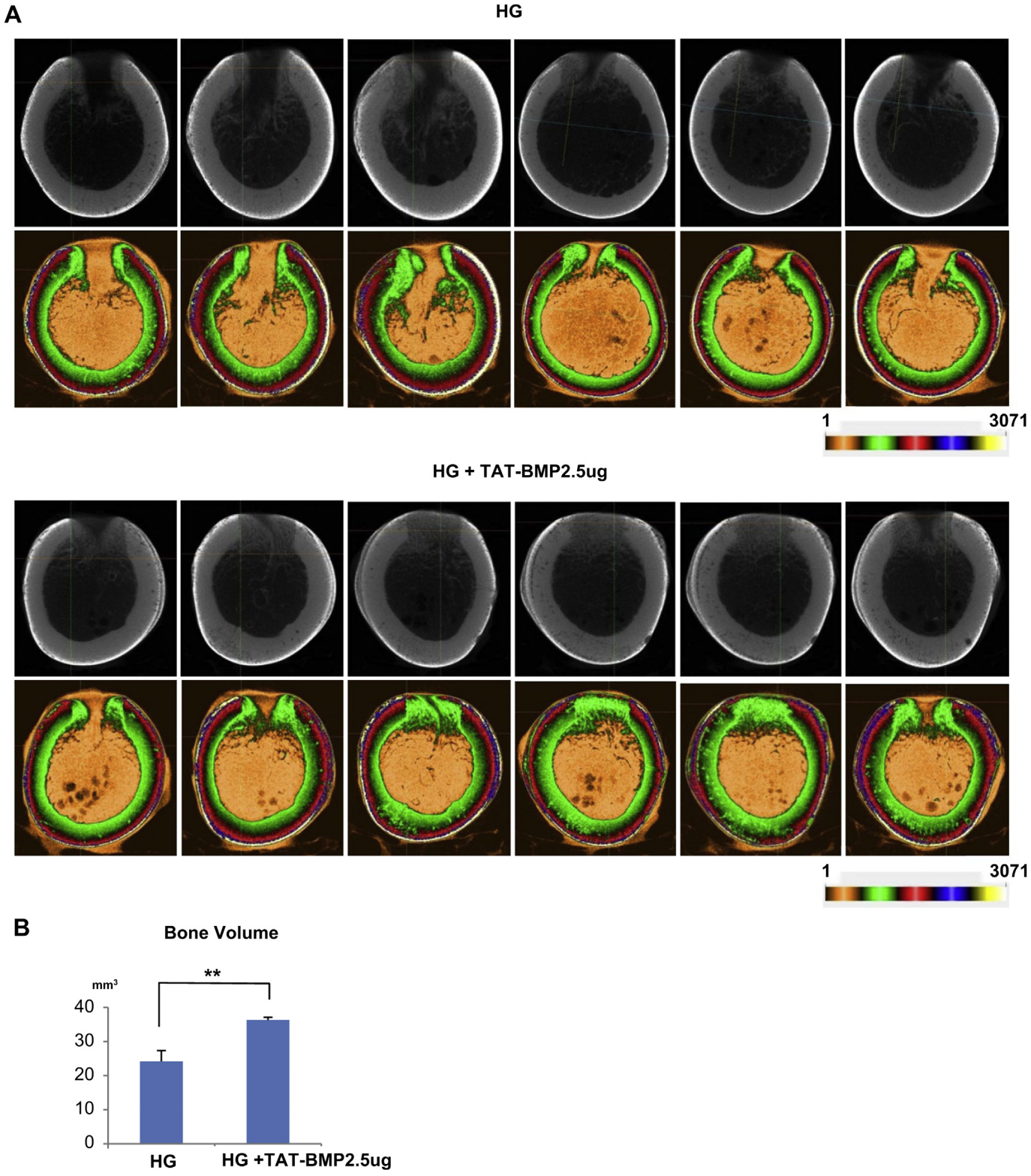

Fig. 4. TAT-BMP-2 is functional for in vivo bone regeneration. (A) Bone regeneration potential by inserting hydrogel only (HG) or HG containing 2.5 μg of TAT-BMP-2 was examined by microCT (black/white images) and through reconstructed color images. Color key on right bottom represents bone density. (B) Regenerate bone volume in the defected area was assessed from 3-D images (**$p < 0.01$).

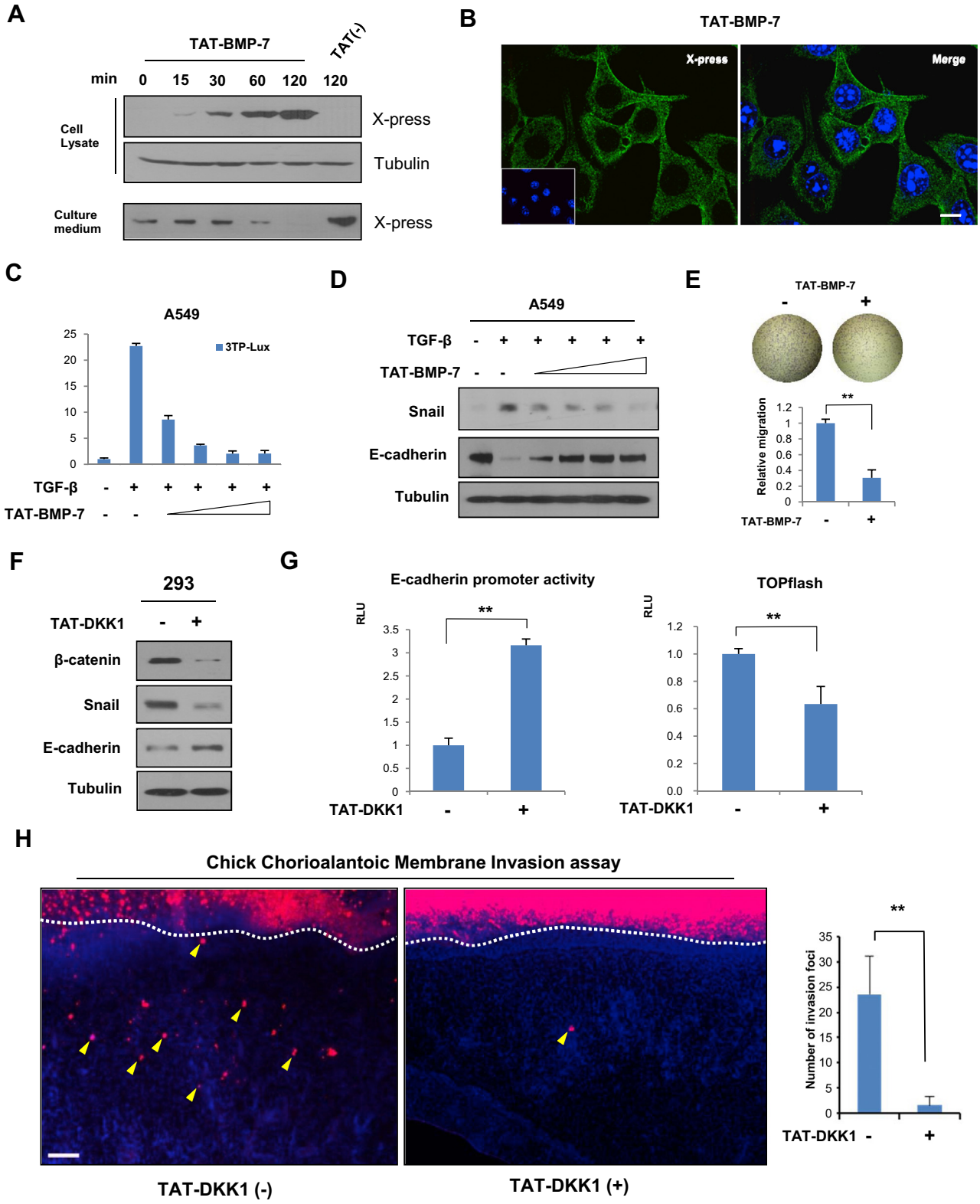

Fig. 5. PTD-mediated protein transduction as a simple platform antagonizing EMT induced by TGF-β or canonical Wnt signaling. (A) Transduction of PTD-recombinant BMP-7 was detected by immunoblot analysis in A549 cells as described in Fig. 1B. (B) The transduction of TAT-BMP-7 recombinant protein (green) was determined by confocal laser microscopy in A549 cells. Nuclei are stained blue with ToTo-3 (inset in left panel). The scale bar in the merged image represents 10 μm. (C) The A549 cells were transfected with 300 ng of TGF-β responsive 3 TP-lux reporter, 5 ng of TGF-β with increasing TAT-BMP-7 doses of 25 ng, 50 ng, 100 ng, and 200 ng being added 24 h prior to lysis. The relative luciferase compared to Renilla activity derived from the 3 TP-Lux reporter construct is depicted. (D) The A549 cells were treated with 5 ng of TGF-β as indicated in combination with 25 ng, 50 ng, 100 ng, and 200 ng of TAT-BMP-7 for 24 h prior to lysis, then analyzed for immunoblot against Snail and E-cadherin. (E) The migratory activity of A549 cells was measured by transwell migration with control or TAT-BMP-7 (100 ng) prior to plating in transwell. Treatment of TAT-BMP-7 largely attenuated the cell migration potential of A549 cells (data are presented as mean ± standard error, $^{**}p < 0.01$). (F) The 293 cells were treated with 100 ng of TAT-DKK-1 for 16 h period, and the expression of β-catenin, Snail, and E-cadherin was analyzed by immunoblot analysis. (G) The 293 cells were transfected with E-cadherin promoter or TCF reporter constructs (TOP/FOP), treated with 10 ng of TAT-DKK-1 for 24 h prior to lysis, and assessed for firefly luciferase activity. The relative activity of wt reporter compared to mutant E-box or TCF/LEF binding sites is depicted. (H) Negative control (−) or 500 ng of TAT-DKK1 (+) transduced in MDA-MB-231 cells were cultured atop the embryonic chick CAM (upper CAM basement membrane surface demarcated by dotted line) and the invasive activity of cancer cells (labeled as dsRed) was monitored by fluorescence microscopy. White arrowheads indicate cancer cell invasion into the parenchyma of CAM tissues. Scale bar, 100 μm. Relative invasive activity of MDA-MB-231 cells is quantified as described in Methods (right panel, $p = 8.43E\text{-}9$).

(Fig. S3). These results suggest that a low μg scale of recombinant TAT-BMP-2 suffices for in vivo osteoinductive potential.

3.5. A platform technique antagonizing the epithelial–mesenchymal transition and canonical Wnt signaling

The EMT, comprising an important cellular mechanism of cancer cell invasion as well as of organ fibrosis [4,6,23,34,35], is modulated by secreted growth factors. The activation of TGF-β and/or the Wnt/Snail axis lead to a loss of cell adhesion via increased protein abundance of Snail, a potent E-cadherin repressor [23,26]. Conversely, BMP-7 can antagonize TGF-β signaling in cells and exogenous BMP-7 can revert EMT accompanied by chronic renal injury [4,36]. Meanwhile, DKK-1 is an endogenous inhibitor antagonizing canonical Wnt [23,37], followed by suppression of β-catenin/TCF and a Snail-mediated transcriptional program. Adenoviral administration of DKK-1 successfully blocks LRP-6-mediated pericyte activation and reverses myofibroblast activation in vivo, resulting in inhibition of multiple fibrogenic signals, capillary rarefaction, and inflammation [38–41]. Extending our approach to the EMT process, we cloned cDNAs of BMP-7 and DKK-1 into the TAT-fusion expression cassette instead of BMP-2. The TAT-BMP-7 recombinant polypeptide was also successfully transduced into the cell in a time- and PTD-dependent manner (Fig. 4, A and B). As BMP-7 acted as an antagonist of TGF-β signaling [4], transduction of TAT-BMP-7 on cells attenuated TGF-β responsive reporter activity (Fig. 5C). Functionally, the recombinant TAT-BMP-7 could revert the TGF-β-induced EMT process in A549 cells by reinducing E-cadherin and suppressing Snail protein abundance in a dose-dependent manner (Fig. 5D). Consistent with reversion of EMT, A549 cell migration potential was largely inhibited by TAT-BMP-7 (Fig. 5E), indicating that TAT-BMP-7 successfully blocks the TGF-β-mediated EMT process. DKK-1 effectively inhibits tissue fibrosis and inflammatory response by blocking multiple EMT-inducing signaling cascades [38,39]. The transduction of TAT-DKK-1 polypeptide was functional in cells, inhibiting the Wnt-mediated EMT program by suppressing Snail and increasing E-cadherin protein abundances (Fig. 5F). Further, transduction of TAT-DKK-1 suppressed β-catenin/TCF transcriptional activity while increasing E-cadherin promoter activity (Fig. 5G). Since DKK-1 overexpression successfully blocked cancer cell invasion on chick CAM (chorioalantoic membrane) in vivo [23], we chose highly invasive MDA-MB-231 cells to test the in vivo proof of concept of TAT-DKK-1. Indeed, transduction of TAT-DKK-1 into MDA-MB-231 cells could largely inhibit the invasive progression of cancer cells through the basement membrane (Fig. 5H). These results demonstrate that our PTD-fusion technique can be easily extended therapeutically to other secreted proteins.

4. Discussion

Growth factors and cytokines comprise a wide range of secreted proteins therapeutically useful in many types of disease. In this study, we show a new MoA of secreted growth factors, mimicking the biogenesis of endogenous proteins. Our indirect delivery strategy using a PTD-protein has several advantages in terms of efficacy and safety compared to current soluble factors. First, sustained delivery of secreted proteins with new MoA overcomes initial burst release because the exposure of TAT-fusion polypeptides into the patient's own progenitor cells depends only on the absorption or degradation of delivery materials. As a denatured polypeptide, the prodrug is also resistant to clearance by body fluid and proteolytic degradation. Second, biological activity of soluble protein is difficult to maintain in vivo during long-term regeneration, whereas the PTD-mediated approach opens up diverse options for carrier/scaffold materials requiring long-term sustained release without consideration of biological activity of the polypeptide. Third, PTD-mediated protein delivery provides a significant safety advantage over current soluble factors. Even with well-designed carriers, the current growth factors required for supra-physiological loading of proteins leak into surrounding tissue with many complications [11,42]. This MoA allows minimum amount of polypeptide for clinical effectiveness while minimizing adverse effects. Fourth, the production cost of current soluble factors remains high despite the availability of bacterial recombinant protein [11]. Our PTD-recombinant protein yields a significant cost advantage in trials involving large internal organs such as kidney, liver, and lung, because the polypeptide is obtained through simple purification of inclusion bodies, a major product of bacterial recombinant culture. Lastly, the novel MoA of our technique makes the platform easily extensible to other secreted growth factors. As EMT controlled by TGF-β and the Wnt/Snail axis appears in many degenerative disorders, chronic inflammatory diseases, and cancer [35,40,41], the technique can be easily adopted to deliver antagonists of TGF-β and Wnt signaling.

5. Conclusion

In this study, we report a simple platform for a prodrug of growth factors with a novel MoA. We have developed a PTD-based recombinant BMP-2 polypeptide to transduce polypeptide into cells followed by furin-mediated protein cleavage and secretion of active growth factor. The PTD-BMP-2 polypeptide was functional for in vivo bone regeneration, only a few micrograms scale being sufficient. Because this MoA mimics endogenous processing of secreted proteins, we have easily extended its application to other growth factors, providing a simple platform for next generation growth factor therapeutics.

Author contributions

N.H.K. constructed all expression vectors used in this study and directed in vitro experiments. Y.H.C., J.K.H., H-J.K., and S.E.L performed animal experiments and image analysis. J.K.R., and Y.L. performed recombinant protein purification and subsequent in vitro experiments. J.K.K. and J.M.K. provided the initial idea and sponsored the project. S.L. and I. N. performed hydrogel composite experiments. X.L. performed immunofluorescence and CAM study. H.S.K., T.A.J., and J.I.Y. conceived the project and wrote the manuscript.

Competing financial interests

J.M.K. and J.K.K. are employees of Ortholution. A patent application describing ideas presented in this paper has been filed by Ortholution (PCT/WO2006/104306 A1 by J.M.K. and J.K.K.). J.M.K. and J.K.K. own stock in Ortholution.

Acknowledgments

We thank E. Tunkle for preparation of the manuscript and professor S. G. Ahn at Chosun University for helpful discussion of PTD technique. This work was supported by grants from the Ortholution and from the National Research Foundation of Korea (NRF-2012M3A9B2052523, NRF-2013R1A1A1011652, NRF-2014R1A2A1A05004670) and from the Seoul R&BD Program (PA110028).

Appendix A. Supplementary data

Supplementary data related to this article can be found at http://dx.doi.org/10.1016/j.biomaterials.2014.08.005.

References

[1] Urist MR, Nakata N, Felser JM, Nogami H, Hanamura H, Miki T, et al. An osteosarcoma cell and matrix retained morphogen for normal bone formation. Clin Orthop Relat Res 1977;124:251–66.
[2] Wozney JM, Rosen V, Celeste AJ, Mitsock LM, Whitters MJ, Kriz RW, et al. Novel regulators of bone formation: molecular clones and activities. Science 1988;242:1528–34.
[3] Samavarchi-Tehrani P, Golipour A, David L, Sung HK, Beyer TA, Datti A, et al. Functional genomics reveals a BMP-driven mesenchymal-to-epithelial transition in the initiation of somatic cell reprogramming. Cell Stem Cell 2010;7:64–77.
[4] Zeisberg M, Hanai J, Sugimoto H, Mammoto T, Charytan D, Strutz F, et al. BMP-7 counteracts TGF-beta1-induced epithelial-to-mesenchymal transition and reverses chronic renal injury. Nat Med 2003;9:964–8.
[5] Wang S, de Caestecker M, Kopp J, Mitu G, Lapage J, Hirschberg R. Renal bone morphogenetic protein-7 protects against diabetic nephropathy. J Am Soc Nephrol 2006;17:2504–12.
[6] Kinoshita K, Iimuro Y, Otogawa K, Saika S, Inagaki Y, Nakajima Y, et al. Adenovirus-mediated expression of BMP-7 suppresses the development of liver fibrosis in rats. Gut 2007;56:706–14.
[7] Zeisberg M, Shah AA, Kalluri R. Bone morphogenic protein-7 induces mesenchymal to epithelial transition in adult renal fibroblasts and facilitates regeneration of injured kidney. J Biol Chem 2005;280:8094–100.
[8] Lieberman JR, Daluiski A, Einhorn TA. The role of growth factors in the repair of bone. Biology and clinical applications. J Bone Jt Surg Am 2002;84-A:1032–44.
[9] Mroz TE, Wang JC, Hashimoto R, Norvell DC. Complications related to osteobiologics use in spine surgery: a systematic review. Spine 2010;35:S86–104.
[10] Poynton AR, Lane JM. Safety profile for the clinical use of bone morphogenetic proteins in the spine. Spine 2002;27:S40–8.
[11] Lo KW, Ulery BD, Ashe KM, Laurencin CT. Studies of bone morphogenetic protein-based surgical repair. Adv Drug Deliv Rev 2012;64:1277–91.
[12] Seeherman H, Wozney JM. Delivery of bone morphogenetic proteins for orthopedic tissue regeneration. Cytokine Growth Factor Rev 2005;16:329–45.
[13] Carragee EJ, Hurwitz EL, Weiner BK. A critical review of recombinant human bone morphogenetic protein-2 trials in spinal surgery: emerging safety concerns and lessons learned. Spine J 2011;11:471–91.
[14] Moatz B, Tortolani PJ. Transforaminal lumbar interbody fusion and posterior lumbar interbody fusion utilizing BMP-2 in treatment of degenerative spondylolisthesis: neither safe nor cost effective. Surg Neurol Int 2013;4:S67–73.
[15] Garrison KR, Donell S, Ryder J, Shemilt I, Mugford M, Harvey I, et al. Clinical effectiveness and cost-effectiveness of bone morphogenetic proteins in the non-healing of fractures and spinal fusion: a systematic review. Health Technol Assess 2007;11:1–150.
[16] Frankel AD, Pabo CO. Cellular uptake of the tat protein from human immunodeficiency virus. Cell 1988;55:1189–93.
[17] van den Berg A, Dowdy SF. Protein transduction domain delivery of therapeutic macromolecules. Curr Opin Biotechnol 2011;22:888–93.
[18] Wadia JS, Stan RV, Dowdy SF. Transducible TAT-HA fusogenic peptide enhances escape of TAT-fusion proteins after lipid raft macropinocytosis. Nat Med 2004;10:310–5.
[19] Nagahara H, Vocero-Akbani AM, Snyder EL, Ho A, Latham DG, Lissy NA, et al. Transduction of full-length TAT fusion proteins into mammalian cells: TAT-p27Kip1 induces cell migration. Nat Med 1998;4:1449–52.
[20] Schwarze SR, Ho A, Vocero-Akbani A, Dowdy SF. In vivo protein transduction: delivery of a biologically active protein into the mouse. Science 1999;285:1569–72.
[21] Schneider C, Sepp-Lorenzino L, Nimmesgern E, Ouerfelli O, Danishefsky S, Rosen N, et al. Pharmacologic shifting of a balance between protein refolding and degradation mediated by Hsp90. Proc Natl Acad Sci U S A 1996;93:14536–41.
[22] Becker-Hapak M, Dowdy SF. Protein transduction: generation of full-length transducible proteins using the TAT system. Curr Protoc Cell Biol 2003.20.2.1–20.2.25.
[23] Yook JI, Li XY, Ota I, Hu C, Kim HS, Kim NH, et al. A Wnt-Axin2-GSK3beta cascade regulates Snail1 activity in breast cancer cells. Nat Cell Biol 2006;8:1398–406.
[24] Park SY, Kim HS, Kim NH, Ji S, Cha SY, Kang JG, et al. Snail1 is stabilized by O-GlcNAc modification in hyperglycaemic condition. EMBO J 2010;29:3787–96.
[25] Pei D, Weiss SJ. Furin-dependent intracellular activation of the human stromelysin-3 zymogen. Nature 1995;375:244–7.
[26] Yook JI, Li XY, Ota I, Fearon ER, Weiss SJ. Wnt-dependent regulation of the E-cadherin repressor snail. J Biol Chem 2005;280:11740–8.
[27] Jo S, Kim S, Noh I. Synthesis of in situ chondroitin sulfate hydrogel through phosphine-mediated Michael type addition reaction. Macromol Res 2012;20:968–76.
[28] Kim NH, Kim HS, Kim NG, Lee I, Choi HS, Li XY, et al. p53 and microRNA-34 are suppressors of canonical Wnt signaling. Sci Signal 2011;4:ra71.
[29] Joliot A, Prochiantz A. Transduction peptides: from technology to physiology. Nat Cell Biol 2004;6:189–96.
[30] Constam DB, Robertson EJ. Regulation of bone morphogenetic protein activity by pro domains and proprotein convertases. J Cell Biol 1999;144:139–49.
[31] Han X, Bushweller JH, Cafiso DS, Tamm LK. Membrane structure and fusion-triggering conformational change of the fusion domain from influenza hemagglutinin. Nat Struct Biol 2001;8:715–20.
[32] Leighton M, Kadler KE. Paired basic/Furin-like proprotein convertase cleavage of Pro-BMP-1 in the trans-Golgi network. J Biol Chem 2003;278:18478–84.
[33] Jean F, Stella K, Thomas L, Liu G, Xiang Y, Reason AJ, et al. alpha1-Antitrypsin Portland, a bioengineered serpin highly selective for furin: application as an antipathogenic agent. Proc Natl Acad Sci U S A 1998;95:7293–8.
[34] Kim NH, Kim HS, Li XY, Lee I, Choi HS, Kang SE, et al. A p53/miRNA-34 axis regulates Snail1-dependent cancer cell epithelial-mesenchymal transition. J Cell Biol 2011;195:417–33.
[35] Henderson Jr WR, Chi EY, Ye X, Nguyen C, Tien YT, Zhou B, et al. Inhibition of Wnt/beta-catenin/CREB binding protein (CBP) signaling reverses pulmonary fibrosis. Proc Natl Acad Sci U S A 2010;107:14309–14.
[36] Boon MR, van der Horst G, van der Pluijm G, Tamsma JT, Smit JW, Rensen PC. Bone morphogenetic protein 7: a broad-spectrum growth factor with multiple target therapeutic potency. Cytokine Growth Factor Rev 2011;22:221–9.
[37] Niehrs C. Function and biological roles of the Dickkopf family of Wnt modulators. Oncogene 2006;25:7469–81.
[38] Mao B, Wu W, Li Y, Hoppe D, Stannek P, Glinka A, et al. LDL-receptor-related protein 6 is a receptor for Dickkopf proteins. Nature 2001;411:321–5.
[39] Ren S, Johnson BG, Kida Y, Ip C, Davidson KC, Lin SL, et al. LRP-6 is a coreceptor for multiple fibrogenic signaling pathways in pericytes and myofibroblasts that are inhibited by DKK-1. Proc Natl Acad Sci U S A 2013;110:1440–5.
[40] Rowe RG, Lin Y, Shimizu-Hirota R, Hanada S, Neilson EG, Greenson JK, et al. Hepatocyte-derived Snail1 propagates liver fibrosis progression. Mol Cell Biol 2011;31:2392–403.
[41] He W, Dai C, Li Y, Zeng G, Monga SP, Liu Y. Wnt/beta-catenin signaling promotes renal interstitial fibrosis. J Am Soc Nephrol 2009;20:765–76.
[42] Smucker JD, Rhee JM, Singh K, Yoon ST, Heller JG. Increased swelling complications associated with off-label usage of rhBMP-2 in the anterior cervical spine. Spine 2006;31:2813–9.